Intermolecular charge transfer enhances two-photon absorption in yellow fluorescent protein†

Maarten T.P. Beerepoot,*[a] Daniel H. Friese[a] and Kenneth Ruud[a]

Received Xth XXXXXXXXXX 20XX, Accepted Xth XXXXXXXXX 20XX
First published on the web Xth XXXXXXXXXX 200X
DOI: 10.1039/b000000x

We present a quantum chemical study of the two-photon absorption (TPA) properties of yellow fluorescent protein (YFP), a mutant of the extensively studied green fluorescent protein. The aromatic chromophore of YFP has a π-stacking interaction with the aromatic ring of a tyrosine residue (Tyr203) in a parellel-displaced structure with a distance of about 3.4 Å. We study the TPA spectrum of the π-stacking system of YFP using the well-established Coulomb-attenuated B3LYP density functional (CAM-B3LYP) and the second-order approximate coupled-cluster model CC2. This work presents both the first comprehensive study of the two-photon absorption spectrum of YFP and the largest-scale coupled-cluster calculation of two-photon absorption that has ever been performed. We analyze the intermolecular charge-transfer (ICT) transitions in this stacked system and show that the ICT transitions are an important mechanism for enhancing the TPA cross sections in YFP. We investigate the distance dependence of the ICT transitions and show that their TPA cross sections are strongly dependent on the separation of the aromatic moieties. This provides a means for tuning the TPA properties of YFP and other structurally related fluorescent proteins through molecular engineering.

1 Introduction

Two-photon absorption (TPA) is a nonlinear optical process with its strength depending on the square of the intensity of the incident light. Although described by Göppert-Mayer already in 1931,[1] the first measurement was only made possible thirty years later due to the high intensity of the light source needed.[2] There are numerous possible applications of TPA and they are as diverse as photodynamic cancer therapy, drug delivery, optical imaging and three-dimensional data storage.[3–5] The development of these applications relies on the quest for molecules with high TPA cross sections at a desirable wavelength.[5,6]

Chakrabarti and Ruud found that intermolecular charge-transfer (ICT) transitions can lead to high TPA cross sections in supermolecular π-stacking systems.[7,8] Indeed, they found that the cooperative effect of two aromatic molecules can tune the absorption wavelength and enhance the TPA cross sections relative to the single substituents in fullerene-buckycatcher[7] and molecular tweezer[8] complexes.

Motivated by the studies of Chakrabarti and Ruud, we wanted to investigate the TPA spectrum of the π-stacking system in yellow fluorescent protein (YFP), a mutant of green fluorescent protein (GFP). GFP and its mutants are popular protein tags in *in vivo* imaging. The chromophore of these fluorescent proteins is an aromatic system consisting of a phenol and an imidazolidone ring with a connecting CH bridge. The *gfp* gene can be incorporated into the genetic code of a host organism and co-expressed with the protein under study to analyse its location and movement in a living cell.[9] In YFP, an aromatic ring was introduced close to the chromophore to create a π-stacking system that red shifts the absorption and excitation wavelength of the protein.[10] Indeed, the crystal structures of YFP show the chromophore and the tyrosine 203 (Tyr203) residue in a parallel-displaced stacking geometry[10,11] (see Figure 1).

From experimental work it is known that the TPA maximum of the lowest excitation in YFP (480 nm[12], 485 nm[13]) is blue-shifted with respect to the one-photon absorption (OPA) maximum by approximately 29[13] to 34[12] nm. Regardless of the type of excitation (OPA or TPA), the excitation maximum is around 530 nm.[13]

The study of absorption properties of fluorescent proteins is usually limited to OPA. TPA of fluorescent proteins has been studied theoretically, but often takes into account only the lowest excitation energy[14–16] and — relevant in the case of YFP — only the chromophore.[17] The π-stacking system of YFP has been studied theoretically in the context of second harmonic generation, another nonlinear optical technique used for optical imaging.[18,19]

The aim of this work is to calculate the TPA spectrum of the chromophore–Tyr203 π-stacking system of YFP and to inves-

[a] *Centre for Theoretical and Computational Chemistry, Department of Chemistry, University of Tromsø, N-9037 Tromsø, Norway. E-mail: maarten.beerepoot@uit.no; Tel.: +47 77623103*

† Electronic Supplementary Information (ESI) available. See DOI: 10.1039/b000000x/

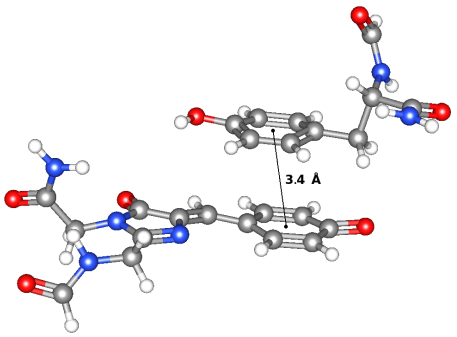

Fig. 1 The molecular structure used in this study: the chromophore of the yellow fluorescent protein (YFP; bottom) and the tyrosine 203 residue (Tyr203; top). The distance between the centres of the phenol rings from the chromophore and Tyr203 is 3.4 Å in the geometry shown.

tigate the character of the involved transitions. We will not limit ourselves to the lowest excitation and instead present a complete calculated TPA spectrum both using DFT with the CAM-B3LYP functional and using the RI-CC2 method. We will demonstrate that intermolecular charge-transfer transitions play an important role in the TPA spectrum. Moreover, we will show that part of the spectrum is affected by the distance between the two rings that make up the aromatic stack. We will demonstrate that calculating a TPA spectrum is possible with the RI-CC2 method also for such big systems and use it to evaluate the performance of DFT. The results provide insights both on the possible use of the TPA of YFP for *in vivo* imaging and for the design of TPA probes with favourable absorption characteristics.

2 Computational details

2.1 Molecular structures

The 1F0B[11] crystal structure of YFP (denoted YFP-H148Q in Ref. 11) was obtained from the protein data bank[20] and prepared with an anionic chromophore as described in Ref. 21. The hydrogen bonding network around the chromophore (CH_2OH in Ser205, COOH in Glu222 and H_2O between Ser205 and phenolate from the chromophore) was relaxed classically (conjugate gradient with convergence to a gradient of 0.05) with the rest of the protein present as a frozen constraint.

The chromophore and parts of its surrounding were subsequently geometry optimized using DFT (B3LYP[22]/6-31+G*[23–25]) within the electrostatic field of the rest of the protein using the QSite QM/MM program.[26] The QM part consisted of i) the conjugated system of the chromophore (using hydrogen caps to cut the bonds to the rest of the protein), ii) six residues involved in hydrogen-bonding with the chromophore: Gln94, Arg96, Gln148, Tyr203, Ser205 and Glu222 (all using frozen orbital cuts between C_α and C_β) and iii) three water molecules that are hydrogen-bonded directly to the chromophore.

The chromophore that was cut out for the two-photon absorption calculations consisted of residues 65-67, including a carbonyl group at the N-terminus and a nitrogen at the C-terminus from residues 64 and 68, respectively, as in earlier work.[14,21] Both sides were capped with an extra hydrogen atom. In the same way, residue Tyr203 was cut out and capped with hydrogen atoms at the linking position to the protein backbone. The structure is shown in Figure 1, the coordinates are given in the Supporting Information.†

In order to understand the relationship between the molecular structure and the TPA spectrum, additional calculations were performed. Several structures were prepared with a varying distance between the centres of the phenol rings of the chromophore and Tyr203 by translating the Tyr203 residue by steps of 0.1 Å along the vector between the centres of the phenol rings while keeping the same coordinates for the chromophore. In this way, the *geometry* of the chromophore and Tyr203 and the *orientation* with respect to each other were the same in all structures, whereas only the *distance* between the aromatic rings varied. The distance between the centres of the phenol rings in two available crystal structures is 3.44 Å for 1F0B[11] and 3.47 Å for 2YFP.[10] The distances are 3.41 Å and 3.38 Å, respectively, after the structure preparation described above, indicating that the distance between the rings is described adequately in the DFT-optimized structure.

2.2 DFT calculations

Vertical excitation energies were calculated with time-dependent DFT using the CAM-B3LYP functional[27] and the aug-cc-pVDZ basis set[28] (1076 basis functions) in Dalton2011.[29] The CAM-B3LYP functional was chosen for its reliability in the treatment of charge-transfer states.[30–32] Since the smaller 6-31+G* basis set[23–25] (716 basis functions) gives qualitatively equivalent results (*vide infra*), this basis set was used for the additional calculations on the stack at different distances (Section 3.2).

2.3 CC2 calculations

The TPA spectrum was also calculated with the approximate second-order coupled-cluster singles and doubles model CC2[33] in combination with the resolution-of-identity (RI) approximation (also referred to as density fitting) for the treatment of the two-electron integrals.[34] This was done using the `ricc2`-module of the TURBOMOLE suite of programs[35] using recently implemented functionality.[32] The RI-CC2 ap-

proach has proven to be a very efficient and reliable tool for the treatment of ground and excited states as well as transition properties.[32,36,37] The Dunning-style basis set aug-cc-pVDZ[28] (1076 basis functions) was used together with the corresponding auxiliary basis sets (3239 basis functions) for the treatment of the two-electron integrals.[38] All 1s-orbitals of the carbon, oxygen and nitrogen atoms were kept frozen in the correlation treatment. The CC2 calculations were performed using an OpenMP parallelization of the code.

D1 diagnostics (0.13) and occupation numbers of the natural HOMO (1.87) indicate possible multireference character of the system under study, questioning the validity of the CC2 method.† This is likely to be related to the two resonance structures of the anionic chromophore, with the negative charge being either on the phenol oxygen or the imidazolidone oxygen. The observation that these numbers are not affected by the distance between the chromophore and Tyr203 (Table SI-X†) indicates indeed that the phenomenon is not an effect of combining the two molecules. However, as bond length alternations in the conjugated system are the same in MP2/cc-pVTZ and B3LYP/6-31+G* optimized structures of the conjugated system in vacuum (data not shown), there is no reason to believe that the description of static correlation in this system is qualitatively wrong in the MP2/CC2 calculations.

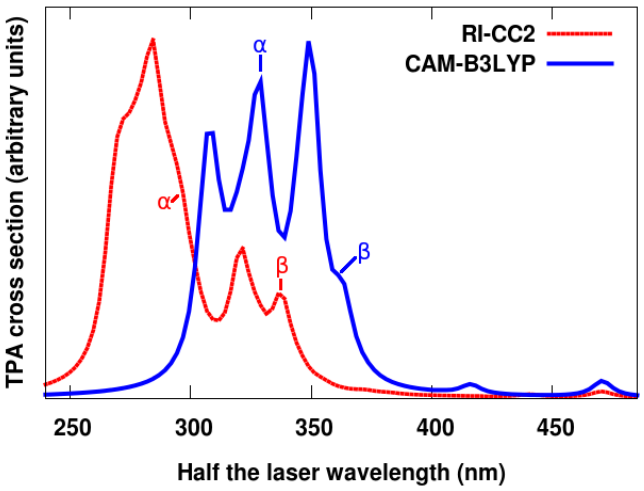

Fig. 2 Comparison of RI-CC2 and CAM-B3LYP calculated two-photon absorption (TPA) spectra, both calculated with the aug-cc-pVDZ basis set. The TPA cross sections have been plotted with a Lorentzian broadening factor of 5 nm for the lowest 35 (RI-CC2) and 20 (CAM-B3LYP) electronic excitations. The spectrum from the DFT calculation has been shifted by +46 nm so that the lowest excitation is at 470 nm for both spectra. The highest cross section has a magnitude of 728 GM for RI-CC2 and 78 GM for CAM-B3LYP† and the cross sections have been scaled to facilitate comparison. Excitations involving one of the main intermolecular charge-transfer transitions are labeled α and β (see Figures 3 and 4).

3 Results

3.1 The calculated TPA spectrum of YFP

The two-photon absorption spectrum of the YFP complex at a distance of 3.4 Å (see Figure 1) has been calculated both with RI-CC2 and CAM-B3LYP and is shown in Figure 2. For RI-CC2 and CAM-B3LYP, the 35 and 20 lowest excitations were calculated, respectively. In order to compare the two spectra, the spectrum obtained with CAM-B3LYP — which is well-known to overestimate excitation energies[21,31,39] — has been shifted by +46 nm so that the lowest excitation (2.636 eV / 470 nm for RI-CC2 and 2.922 eV / 424 nm for CAM-B3LYP) is at the same wavelength for RI-CC2 and CAM-B3LYP. The shortest wavelength transition calculated is 269 nm for RI-CC2 and 259 nm (305 nm after shifting) for CAM-B3LYP, the spectra are therefore not to be interpreted for shorter wavelengths. All calculated excitation energies, one-photon transition strengths and TPA cross sections for RI-CC2 and CAM-B3LYP are reported in the Supporting Information (Tables SI-III and SI-II, respectively†).

Figure 2 shows that the strongest TPA transitions are below 370 nm (below 320 nm for CAM-B3LYP without shifting the spectrum). Some of the strongest transitions are intermolecular charge-transfer (ICT) transitions. We can clearly identify two types of ICT transitions involving the aromatic rings of both species: In the first type, charge is transferred from the phenol ring of Tyr203 to the conjugated system of the chromophore. We denote this transition as ICT-α (see Figure 3). In the second type, charge is transferred from the conjugated system of the chromophore to the phenol ring of Tyr203. We denote this transition as ICT-β (see Figure 4). The HF and KS orbitals involved in these transitions bear a striking resemblance (see Figures SI-1 and SI-2†).

All other strong TPA transitions are Rydberg transitions. Indeed, Rydberg transitions make up the 285 and 321 nm peaks of the RI-CC2 spectrum and the 350 and 308 nm peaks of the CAM-B3LYP spectrum in Figure 2. Moreover, minor Rydberg orbital transitions contribute to all peaks assigned α and β in Figure 2. The stronger Rydberg transitions involve the HOMO on the chromophore and different virtual orbitals located mainly around the amide groups of the chromophore and Tyr203. The transitions are therefore both *intra*molecular and *inter*molecular Rydberg transitions (see Figure SI-3†).

The calculated CAM-B3LYP TPA spectrum of the chromophore without Tyr203 (Figure SI-4†) lacks a strong peak around 283 nm (the ICT-α peak at 329 nm peak in Figure 2). Indeed, intramolecular Rydberg transitions and intramolecular charge transfer transitions involving orbitals on the conjugated system are the only main contributors to the strongest peaks in

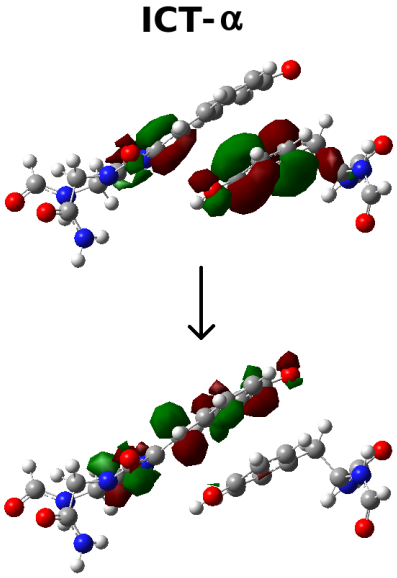

Fig. 3 Hartree-Fock orbitals of the intermolecular charge-transfer transition α (ICT-α) in Figure 2.† Orbital plots are made with Gaussview.[40]

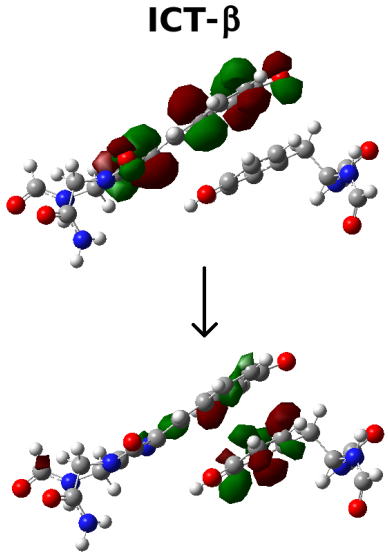

Fig. 4 Hartree-Fock orbitals of the intermolecular charge-transfer transition β (ICT-β) in Figure 2.† Orbital plots are made with Gaussview.[40]

the TPA spectrum of the chromophore.

We note that the number of Rydberg states found is higher with RI-CC2 than with CAM-B3LYP. In particular, the transition denoted as ICT-α is a transition into the LUMO+1 for CAM-B3LYP and into LUMO+19 for RI-CC2. It should be observed that the two orbitals involved are qualitatively equivalent (see Figure SI-1†) and that all the HF orbitals between the HOMO and LUMO+19 are Rydberg orbitals. The higher number of transitions into Rydberg states for CC2 is also the reason why more electronic excitations need to be computed for CC2 (35) than for CAM-B3LYP (20) to describe the same ICT transitions. Differences in orbital ordering were also found in an earlier study where CAM-B3LYP and CC2 were studied using the same basis sets.[32]

The electron density of the Rydberg states will be compressed in the constrained environment of the protein, yielding a much higher energy. Rydberg transitions are therefore an artefact of including only the π-stacking system in our model and we focus on the ICT transitions in this work.

The TPA cross sections calculated with RI-CC2/aug-cc-pVDZ are approximately one order of magnitude higher than those calculated with CAM-B3LYP/aug-cc-pVDZ. In particular, the highest cross section in RI-CC2 is 728 GM (Table SI-III†) and in CAM-B3LYP/aug-cc-pVDZ 78 GM (Table SI-II†). Note that the height of the peaks in Figure 2 may be determined by the cross section of more than one electronic excitation and that each electronic excitation is described by more than one orbital transition. Comparison of the heights of the peaks should therefore be done with caution.

CAM-B3LYP calculations with the smaller 6-31+G* basis set give qualitatively similar results. Indeed, the orbitals involved in the ICT-α (Figure SI-1†) and ICT-β transitions (Figure SI-2†) show high similarity with the Kohn–Sham orbitals obtained with the larger aug-cc-pVDZ basis set. The main differences are the higher TPA cross sections and the lower number of Rydberg states for the 6-31+G* basis (Tables SI-I and SI-II†). Since our focus is a qualitative description of the spectrum rather than a quantitative one, we use the 6-31+G* basis for the additional calculations on the distance between the stacks.

3.2 Distance dependence of the ICT transitions

To investigate the dependence of the ICT transitions on the molecular geometry, the CAM-B3LYP TPA spectrum has been calculated for the chromophore–Tyr203 stack at different intermolecular distances. The spectra are shown in Figures 5.

Part of the TPA spectrum is notably affected by the distance between the two aromatic molecules. All ICT transitions are red shifted when decreasing the distance between the chromophore and Tyr203 (see Section SI-4†). In addition, the intensity of the ICT-α transition around 280 nm is clearly correlated with the proximity of the two moieties (Tables SI-VI†). We note, however, that the orbital transitions contributing to these peaks are not the same. For the structure at 3.3 Å, Rydberg transitions and an *intra*molecular charge-transfer transition on the chromophore contribute to the peak at 284 nm. For the structures at 3.4 and 3.5 Å, Rydberg transitions and

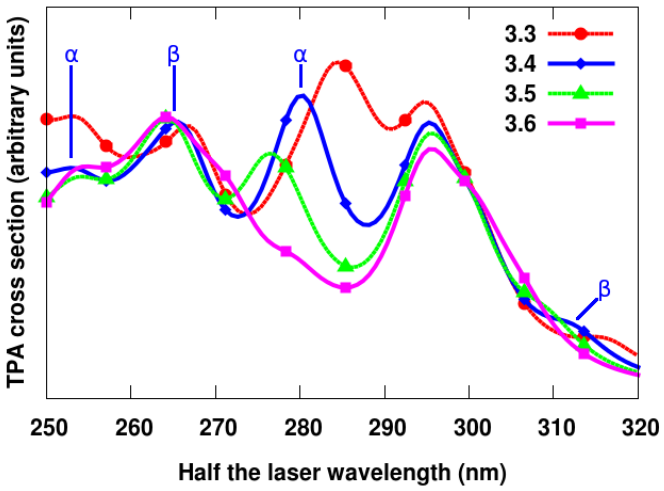

Fig. 5 Calculated CAM-B3LYP/6-31+G* two-photon absorption (TPA) spectra of the chromophore and Tyr203 from yellow fluorescent protein at various intermolecular distances (see Figure 1 for the structure). The different lines refer to a different distance (in Å) between the centre of the phenol rings of the chromophore and Tyr203. The TPA cross sections have been plotted with a Lorentzian broadening factor of 5 nm for the lowest 20 electronic excitations. The wavelengths have not been shifted as in Figure 2. The main intermolecular charge-transfer transitions are labeled α and β (see Figures 3 and 4).

ICT-α (see Figure 3) contribute to the peaks at 279 and 276 nm. For the structure at 3.6 Å, the ICT-α transition at 272 nm is merely a shoulder to the ICT-β transition at 264 nm. The distance dependence of the *spectral peak* is therefore not equivalent to the distance dependence of the *electronic excitation*. Moreover, comparison is not straightforward because different *orbital transitions* contribute to different extent to the *electronic excitations*.

The main trends are qualitatively reproduced by the RI-CC2 calculations: a red shift of all intermolecular charge-transfer transitions when decreasing the distance and a strong dependence of the intensity of especially the ICT-α transitions on the distance between the molecules (Table SI-VII†). To keep the computational effort within bounds, only the TPA cross sections for the lowest excitation and those involving ICT-α and ICT-β were calculated with CC2 (see Tables SI-V, SI-VII and SI-IX†). We stress again that direct comparison of the DFT and CC2 results (and between the structures at different distances) has to be done with caution because of the different orbital transitions that contribute to each electronic excitation.

TPA spectra of the π-stacking system at even longer distances contain fewer and smaller peaks due to the decrease of the strength of intermolecular transitions (Figure SI-5†). Indeed, ICT-α and ICT-β transitions are very weak at a distance of 4.1 Å and completely absent at a distance of 7.1 Å. The main contributions to the peaks in the spectra of the stack at longer separations are Rydberg transitions and intramolecular charge transfer transition involving orbitals on the conjugated system of the chromophore.

4 Discussion

There are two important observations that can be made from our results. First, the lowest excitation in YFP is by far not the one with the highest TPA cross section (see Figure 2 and Tables SI-I to SI-III†). Studying only the lowest excitation — which in fluorescent proteins is the only one with a significant one-photon oscillator strength — will therefore likely hide the interesting two-photon absorption bands, as previously pointed out by Nifosí and Luo.[17] Second, no clear donor and acceptor can be identified in the ICT transition in the π-stacking system studied here. Indeed, Tyr203 serves as the donor and the chromophore as the acceptor in the ICT-α transition (Figures 3 and SI-1†), whereas the roles are inversed for the ICT-β transition (Figures 4 and SI-2†) where the chromophore is the donor and Tyr203 is the acceptor in the charge-transfer transition. This is in contrast to earlier work by Chakrabarti and Ruud on ICT transitions in different π-stacking systems where one of the species could clearly be identified as the donor and the other as the acceptor.[7,8]

Our calculations demonstrate that large-scale coupled-cluster TPA calculations are feasible on medium-sized molecular systems. Indeed, this is to our knowledge the largest coupled-cluster calculation of two-photon absorption performed to date. The YFP complex considered here has 62 atoms and was treated with the aug-cc-pVDZ basis set using a total of 1076 spherical basis functions. CC2 calculations are becoming more common for calculating absorption properties in biological systems. Recently, Kaila *et al.* reported RI-CC2 one-photon absorption calculations — considerably less time consuming than two-photon absorption — on a cluster around the GFP chromophore, including 161 atoms and using the def2-TZVP basis set.[41] Even bigger system can be treated with multiscale methods such as the PERI-CC2 methods of Schwabe *et al.*,[42] which is currently limited to excitation energies and oscillator strengths.

Overall, we can say that the results from CAM-B3LYP and RI-CC2 are in good qualitative agreement. Indeed, the same two ICT transitions are found in the spectra calculated with the two methods (see Figures 2 to 4) and the main orbital contributions show striking similarities (see Figures SI-1 and SI-2†). We can therefore state that CAM-B3LYP is well capable of describing intermolecular charge-transfer transitions, in agreement wirh earlier benchmarking work.[32] We stress the significant difference in the computational time needed to obtain the CAM-B3LYP and CC2 data reported here: for the for-

mer, the whole spectrum reported in Figure 2 was obtained in the order of one day on one node with 12 cores, whereas every single one of the 35 TPA cross sections with the latter method took 1–2 weeks to calculate on one node on the same machine. We therefore suggest for further work to use the DFT with the CAM-B3LYP functional to investigate whether ICT plays a role in a certain system and reserve coupled-cluster calculations for quantitative results on the systems that have been shown to be promising.

The observed red shift in the ICT transitions when the chromophore and Tyr203 approach each other can be explained in terms of orbital relaxation. The red shift is also observed for the lowest excitation (see Tables SI-IV and SI-V†), which is a π-π^* transition with both orbitals involved delocalized over the conjugated system of the chromophore. In fact, this red shift has been explained by taking into account the net charge transfer from the phenol oxygen to the conjugate system of the chromophore in the π-π^* transition. The electronically excited state is then stabilized by the additional polarizability of Tyr203, explaining the observed red shift.[10] The virtual orbital in the ICT-α transitions (see Figure 3) is the same as for the π-π^* transition on the chromophore, which explains the red shift in ICT-α (see Tables SI-VI and SI-VII†). In ICT-β the effect is opposite: the polarizability of the chromophore stabilizes the virtual orbital on Tyr203 leading to a red shift for ICT-β as well (see Tables SI-VIII and SI-IX†).

Comparison with experiment is difficult for the ICT transitions, partly because experiment focuses on longer wavelengths only. Indeed, Spiess *et al.*[13] do not report wavelengths below 435 nm (λ_{laser} = 870 nm) and Blab *et al.*[12] not below 375 nm (λ_{laser} = 750 nm) for the TPA spectrum of YFP. Drobizhev *et al.* report the TPA spectrum of Citrine (an optimized YFP variant) down to 600 nm.[43] The spectrum shows more peaks in the 300 to 400 nm range (600 nm $< \lambda_{laser} <$ 800 nm) than related fluorescent proteins that do not contain Tyr203 (e.g. EGFP, EBFP and ECFP), which could indicate that Tyr203 is directly involved in the excitations. However, a direct comparison with the ICT transitions found in this work is not possible because the calculations do not include the explicit effect of the protein environment and the experimental spectra do not shed light on the nature of the excitations.

The enhancement of the TPA absorption cross section by ICT transitions could make YFP a suitable fluorescent tag for *in vivo* multiphoton imaging applications when excited at the right wavelength. Although the TPA cross sections (see Tables SI-I to SI-III†) of the YFP complex are not as high as other reported TPA probes,[5,7,8] an important advantage is that YFP is already in use in bioimaging applications. YFP has the potential to combine the advantages of fluorescent proteins (non-invasive imaging due to the ease of incorporation into the genetic code of the host organism through molecular genetics) with the advantages of multiphoton excitation (deeper penetration into tissue and less phototoxicity due to longer wavelengths and intrinsic three-dimensional resolution).[4] In particular, the longer wavelength of the laser beam in two-photon excitation (double the wavelength needed for one-photon absorption) prevents loss of resolution due to absorption of light by aromatic amino acids.

This study has only described the main transitions in the supermolecular complex formed by the anionic chromophore and Tyr203 from YFP. We would like to point out that we have not considered the protein environment explicitly in our model system. This is likely to suppress the Rydberg transitions and to influence both the exact location and the strength of each of the electronic excitations.[14] Moreover, non-Condon effects were not taken into account in our vertical transition treatment, although they have been shown to affect TPA in a significant way.[44] Furthermore, we have not sampled the different possible conformations of the complex as can be done e.g. by molecular dynamics and instead focused on the crystal structure.[21] Finally, we have reported *artificial* spectra based on peak locations and intensities using a constant broadening factor of 5 nm, without the information that can be obtained from experimental peak shapes. Despite these limitations, this study does suggest that ICT transitions enhance two-photon absorption cross sections in YFP.

5 Concluding remarks and outlook

We have described how intermolecular charge-transfer transitions enhance the two-photon absorption cross section in the π-stacking system of the yellow fluorescent protein. These transitions occur at shorter wavelength and with a considerably higher two-photon absorption cross section than the only excitation with significant one-photon oscillator strength. Moreover, we have found that CAM-B3LYP and RI-CC2 are in qualitative agreement in the description of the intermolecular charge-transfer transitions, thereby showing that the former is an effective tool for evaluating whether intermolecular charge transfer plays a role in enhancing the TPA cross section in a molecular system. Furthermore, we have shown that part of the two-photon absorption spectrum is sensitive to changes in the distance between the two aromatic systems, demonstrating that tuning of the two-photon absorption properties by molecular engineering is possible.

An interesting point to investigate in more detail in future work is how the ICT transitions depend on the distance between the donor and the acceptor. Thorough knowledge of this can help design strong TPA probes with high absorption cross sections at desirable wavelengths. Moreover, other fluorescent proteins with π-stacking chromophores could be considered to see whether ICT transitions play a role, such as the recently developed SHardonnay.[19] Another interesting direction is the investigation of π-stacking systems containing three aromatic

rings such as the molecular tweezer complex[8] or the recently described triple-decker structure based on YFP.[45] An interesting question is under what conditions a triple stack leads to a higher TPA cross section. Finally, an important contribution to computational work on two-photon absorption would be to investigate the influence of the surrounding (e.g. protein, solvent) on the ICT transitions in combination with sampling of the conformational space. Including the protein environment is possible in an accurate way with the polarizable embedding density functional theory (PE-DFT) method as shown in Ref. 14. This will allow a much better comparison between calculated and measured spectra.

The results presented here have clearly demonstrated that in future work on the TPA of YFP and structurally related fluorescent proteins, at least the chromophore and Tyr203 (or other close-lying aromatic amino acids) should be described by quantum mechanics and that an analysis of only the lowest excitation is not sufficient.

Acknowledgements

This work has received support from the Research Council of Norway through a Centre of Excellence Grant (Grant No. 179568/V30), from the European Research Council through a Starting Grant (Grant No. 279619) to K. R. and from the Norwegian Supercomputer Program (Grant No. nn4654k). The authors thank Prof. Peter R. Taylor (Melbourne) for helpful discussions.

References

1 M. Göppert-Mayer, *Ann. Phys.-Berlin*, 1931, **401**, 273–294.
2 W. Kaiser and C. G. B. Garrett, *Phys. Rev. Lett.*, 1961, **7**, 229–231.
3 W. R. Zipfel, R. M. Williams and W. W. Webb, *Nat. Biotechnol.*, 2003, **21**, 1369–1377.
4 F. Helmchen and W. Denk, *Nat. Methods*, 2005, **2**, 932–940.
5 M. Pawlicki, H. A. Collins, R. G. Denning and H. L. Anderson, *Angew. Chem. Int. Ed.*, 2009, **48**, 3244–3266.
6 F. Terenziani, C. Katan, E. Badaeva, S. Tretiak and M. Blanchard-Desce, *Adv. Mater.*, 2008, **20**, 4641–4678.
7 S. Chakrabarti and K. Ruud, *J. Phys. Chem. A*, 2009, **113**, 5485–5488.
8 S. Chakrabarti and K. Ruud, *Phys. Chem. Chem. Phys.*, 2009, **11**, 2592–2596.
9 R. Y. Tsien, *Annu. Rev. Biochem.*, 1998, **67**, 509–544.
10 R. M. Wachter, M.-A. Elsliger, K. Kallio, G. T. Hanson and S. J. Remington, *Structure*, 1998, **6**, 1267–1277.
11 R. M. Wachter, D. Yarbrough, K. Kallio and S. J. Remington, *J. Mol. Biol.*, 2000, **301**, 157–171.
12 G. A. Blab, P. H. M. Lommerse, L. Cognet, G. S. Harms and T. Schmidt, *Chem. Phys. Lett.*, 2001, **350**, 71–77.
13 E. Spiess, F. Bestvater, A. Heckel-Pompey, K. Toth, M. Hacker, G. Stobrawa, T. Feurer, C. Wotzlaw, U. Berchner-Pfannschmidt, T. Porwol and H. Acker, *J. Microsc.*, 2005, **217**, 200–204.
14 A. H. Steindal, J. M. H. Olsen, K. Ruud, L. Frediani and J. Kongsted, *Phys. Chem. Chem. Phys.*, 2012, **14**, 5440–5451.
15 N. H. List, J. M. H. Olsen, H. J. Aa. Jensen, A. H. Steindal and J. Kongsted, *J. Phys. Chem. Lett.*, 2012, **3**, 3513–3521.
16 M.-Y. Zhang, J.-Y. Wang, C.-S. Lin and W.-D. Cheng, *Int. J. Quantum Chem.*, 2012, **112**, 2607–2614.
17 R. Nifosì and Y. Luo, *J. Phys. Chem. B*, 2007, **111**, 14043–14050.
18 E. De Meulenaere, I. Asselberghs, M. de Wergifosse, E. Botek, S. Spaepen, B. Champagne, J. Vanderleyden and K. Clays, *J. Mat. Chem.*, 2009, **19**, 7514–7519.
19 E. De Meulenaere, N. N. Bich, M. de Wergifosse, K. Van Hecke, L. Van Meervelt, J. Vanderleyden, B. Champagne and K. Clays, *J. Am. Chem. Soc.*, 2013, **135**, 4061–4069.
20 H. M. Berman, J. Westbrook, Z. Feng, G. Gilliland, T. N. Bhat, H. Weissig, I. N. Shindyalov and P. E. Bourne, *Nucl. Acids Res.*, 2000, **28**, 235–242.
21 M. T. P. Beerepoot, A. H. Steindal, J. Kongsted, B. O. Brandsdal, L. Frediani, K. Ruud and J. M. H. Olsen, *Phys. Chem. Chem. Phys.*, 2013, **15**, 4735–4743.
22 A. D. Becke, *J. Chem. Phys.*, 1993, **98**, 5648–5652.
23 W. J. Hehre, R. Ditchfield and J. A. Pople, *J. Chem. Phys.*, 1972, **56**, 2257–2261.
24 M. M. Francl, W. J. Pietro, W. J. Hehre, J. S. Binkley, M. S. Gordon, D. J. DeFrees and J. A. Pople, *J. Chem. Phys.*, 1982, **77**, 3654–3665.
25 T. Clark, J. Chandrasekhar, G. W. Spitznagel and P. V. R. Schleyer, *J. Comput. Chem.*, 1983, **4**, 294–301.
26 QSite, version 5.7, Schrödinger, LLC, New York, NY, 2011.
27 T. Yanai, D. P. Tew and N. C. Handy, *Chem. Phys. Lett.*, 2004, **393**, 51–57.
28 T. H. Dunning, *J. Chem. Phys.*, 1989, **90**, 1007–1023.
29 DALTON, a molecular electronic structure program, Release Dalton2011 (2011), see http://daltonprogram.org/.
30 M. J. G. Peach, P. Benfield, T. Helgaker and D. J. Tozer, *J. Chem. Phys.*, 2008, **128**, 044118.
31 N. H. List, J. M. Olsen, T. Rocha-Rinza, O. Christiansen and J. Kongsted, *Int. J. Quantum Chem.*, 2012, **112**, 789–800.
32 D. H. Friese, C. Hättig and K. Ruud, *Phys. Chem. Chem. Phys.*, 2012, **14**, 1175–1184.
33 O. Christiansen, H. Koch and P. Jørgensen, *Chem. Phys. Lett.*, 1995, **243**, 409–418.
34 C. Hättig and F. Weigend, *J. Chem. Phys.*, 2000, **113**, 5154–5161.
35 *TURBOMOLE developer's version, a development of University of Karlsruhe and Forschungszentrum Karlsruhe GmbH, 1989-2007, TURBOMOLE GmbH, since 2007; available from* `http://www.turbomole.com`.
36 C. Hättig and A. Köhn, *J. Chem. Phys.*, 2002, **117**, 6939–6951.
37 T. B. Pedersen, A. M. J. S. de Merás and H. Koch, *J. Chem. Phys.*, 2004, **120**, 8887–8897.
38 F. Weigend, A. Köhn and C. Hättig, *J. Chem. Phys.*, 2002, **116**, 3175–3183.
39 P. Amat and R. Nifosì, *J. Chem. Theory Comput.*, 2013, **9**, 497–508.
40 GaussView, Version 5, Dennington, R.; Keith, T.; Millam, J. Semichem Inc., Shawnee Mission KS, 2009..
41 V. R. I. Kaila, R. Send and D. Sundholm, *Phys. Chem. Chem. Phys.*, 2013, **15**, 4491–4495.
42 T. Schwabe, K. Sneskov, J. M. H. Olsen, J. Kongsted, O. Christiansen and C. Hättig, *J. Chem. Theory Comput.*, 2012, **8**, 3274–3283.
43 M. Drobizhev, N. S. Makarov, S. E. Tillo, T. E. Hughes and A. Rebane, *Nat. Methods*, 2011, **8**, 393–399.
44 E. Kamarchik and A. I. Krylov, *J. Phys. Chem. Lett.*, 2011, **2**, 488–492.
45 B. L. Grigorenko, A. V. Nemukhin, I. V. Polyakov and A. I. Krylov, *J. Phys. Chem. Lett.*, 2013, **4**, 1743–1747.

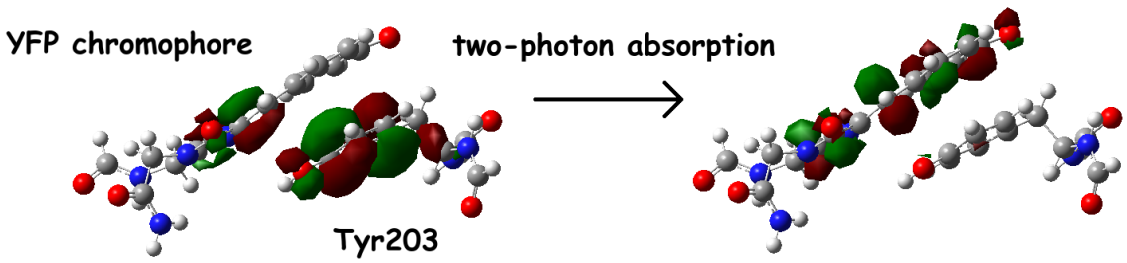

Fig. 6 Intermolecular charge transfer has been found to be an important mechanism for enhancing the two-photon absorption cross sections in the π-stacking system of the chromophore and tyrosine residue 203 (Tyr203) in yellow fluorescent protein (YFP).